2019-07-20

Putting the silicon cycle in a bag: Field and mesocosm observations of silicon isotope fractionation in subtropical waters east of New Zealand

Meyerink, SW

10.1016/j.marchem.2019.04.008
Marine Chemistry
Elsevier

Putting the silicon cycle in a bag: Field observations of silicon isotope fractionation in subtropical waters east of New Zealand

Scott W. Meyerink[1#], Philip W. Boyd[2,3], William A. Maher[4], Angela Milne[5], Robert Strzepek[2,3] and Michael J. Ellwood[1#]

1. Research School of Earth Sciences, Australian National University, Canberra, Australia

2. Department of Chemistry, NIWA/University of Otago Research Centre for Oceanography, University of Otago, Dunedin, New Zealand

3. Now at: Institute for Marine and Antarctic Studies and Antarctic Climate and Ecosystems Co-operative Research Centre, University of Tasmania, Hobart, Australia

4. Ecochemistry Laboratory, Institute for Applied Ecology, University of Canberra, Bruce, Australia.

5. School of Geography, Earth and Environmental Sciences, University of Plymouth, Plymouth PL4 8AA, United Kingdom

corresponding authors: scott.meyerink@anu.edu.au; michael.ellwood@anu.edu.au

Abstract

A mesocosm experiment was used to investigate the fractionation of silicon (Si) isotopes in subtropical surface waters east of New Zealand. This region surface waters were characterised by relatively low concentrations of silicic acid ($Si(OH)_4$) (~2 µmol L^{-1}) and higher nitrate (~5 µmol L^{-1}) and dissolved iron (Fe) concentrations (~0.4 nmol L^{-1}) prior to development of the annual springtime phytoplankton bloom. To simulate initiation of the bloom, a large (~700 L) mesocosm experiment was undertaken whereby surface seawater containing the natural plankton community was incubated for a 168-hr period. During the mesocosm experiment the concentrations of $Si(OH)_4$, nitrate, phosphate and dissolved iron all decreased while the concentration of biogenic silica (BSi) increased 12-fold. Coupled with the increase in BSi was a change in the Si-isotope composition of BSi ($\delta^{30}Si_{BSi}$) which increased from 1.49 ‰ to 2.64 ‰ after 168 hr. Complementary observations to those made for the mesocosm experiment were made for corresponding surface waters. For these waters we observed a small decline in the concentrations of nitrate, phosphate and dissolved Fe, but little change in the concentrations of $Si(OH)_4$ and BSi. In contrast to the mesocosm experiment, surface water $\delta^{30}Si_{BSi}$ values became lighter during bloom initiation, suggestive of $Si(OH)_4$ being replenished into surface waters. These differences in the drawdown and utilisation of nutrients and dissolved Fe between the mesocosm and surface waters during bloom initiation likely result from favourable Fe and light supply conditions within the mesocosm. In contrast, water column stability (i.e. vertical mixing), and the supply of dissolved Fe are likely to influence bloom initiation and its longevity. The fractionation of Si-isotopes in the mesocosm experiment followed closed-system Rayleigh fractionation kinetics, and an enrichment factor (ε) of -1.13 ‰ was calculated for the exponential phase of growth for the diatom community, which was marked by the presence of the diatoms *Asterionelopsis glacilis* and *Mellosira moniliformis*. The isotope enrichment factor agreed well with previous observations of Si isotope fraction in diatoms from field communities, and appeared to be independent of variations in the ambient $Si(OH)_4$ concentration, and phytoplankton species composition.

1. Introduction

The biological fractionation of silicon (Si) isotopes by diatoms in the surface ocean makes the stable isotope composition of biogenic silica ($\delta^{30}Si_{BSi}$) an extremely sensitive tracer of the marine biogeochemical Si-cycle (de Souza et al., 2012b; Sutton et al., 2018). Understanding the processes governing Si-isotope fractionation is particularly important in the Southern Ocean, a region where silicic acid ($Si(OH)_4$) is retained as a result of diatoms in sub-polar waters preferentially removing $Si(OH)_4$ relative to nitrate (NO_3^-) from the water column. These Si-poor waters extend northward as Sub-Antarctic Mode Water (SAMW) and play a significant role in setting the nutrient status of the global ocean (Sarmiento et al., 2004). The strong de-coupling of $Si(OH)_4$ and NO_3^- in Antarctic polar waters has a particularly important bearing on marine productivity at lower latitudes, and is due to a complex interplay between, (1) different diatom species and morphological types displaying varying degrees of bio-silicification (Baines and Pace, 1991), (2) Fe and light limitation inducing heavier rates of bio-silicification and reduced uptake of NO_3^- in diatoms (Brzezinski et al., 2002; Franck et al., 2003; Marchetti et al., 2010), (3) the export and deep remineralisation of $Si(OH)_4$ relative to NO_3^- (Pichevin et al., 2014; Sarmiento et al., 2007), and (4) grazer induced variations in cell wall bio-silicification and cell morphology (Smetacek et al., 2004). Deciphering the relative importance of these processes is key to understanding the nutrient distribution in and outside of the Southern Ocean (Sarmiento et al., 2004).

The distribution of $\delta^{30}Si_{BSi}$ is extremely sensitive to these processes and acts as a useful tracer for examining the cycling of Si in resident diatom communities (De La Rocha et al., 1997; Fripiat et al., 2012; Milligan et al., 2004). The uptake of $Si(OH)_4$ by diatoms in the ocean influences the isotopic compositions of both $Si(OH)_4$ and biogenic silica (BSi) in surface waters. During $Si(OH)_4$ uptake, the lighter Si isotope (^{28}Si) is preferentially taken up, and is defined by a fractionation factor (ε). For laboratory cultures and field populations of diatoms ε generally ranges between -0.53 and -1.9 ‰, with the odd individual species having more extreme values e.g. *Chaetoceros brevis* (Cardinal et al., 2007; De La Rocha et al., 1997; Fripiat et al., 2011; Meyerink et al., 2017; Sutton et al., 2013; Varela et al., 2004). In general, the factors that influence Si silicon isotope fractionation during a phytoplankton bloom formation are not well characterised. The aim of this study was to simulate the formation of the annual spring bloom using mesocosm approach and complement mesocosm observations with water column measurements.

This study took place within a warm-core eddy (39°20S 180°00'W) east of New Zealand where an annual spring phytoplankton bloom has been observed to occur based on satellite and field measurements (Boyd et al., 2012; Ellwood et al., 2015; Murphy et al., 2001). The region is a site of considerable eddy activity, which arises from the convergence of SubAntarctic Water (SAW) and Sub-Tropical Water (STW) (Bostock et al., 2013; Butler et al., 1992; Fernandez et al., 2014). The convergence zone is locked topographically to the Chatham Rise, a shallow (<300 m deep) submarine ridge, and is a region of high temperature, salinity and nutrient gradients as a result of the confluence of two significantly different water masses (SAW and STW) (Chiswell et al., 2015; Nodder et al., 2005). A warm core eddy immediately north of the Chatham Rise is a persistent feature in the region, which extends to 2000 m depth; and has been observed to have a spring bloom at its centre, which induces oligotrophic conditions in summer, and is followed by deep winter mixing and low productivity in winter (Murphy et al., 2001; Nodder et al., 2005). Phytoplankton community structure in the bloom is generally characterised by chlorophyll (Chl) concentrations >1 mg m^{-3}, and large phytoplankton (>20 μm) (Boyd et al., 2012). Consequently, the area is marked by high seasonal fluxes of biogenic material to deeper waters (Nodder et al., 2005; Nodder and Northcote, 2001).

The relatively low concentrations of $Si(OH)_4$ (~2 μmol L^{-1}) compared to NO_3^- (~4 μmol L^{-1}) in surface-ocean waters testify to the influence of SAW in the region (Boyd et al., 1999). A number of Fe-process studies have been undertaken in the region (e.g. (Boyd et al., 2012; Boyd et al., 2015; Ellwood et al., 2015). These studies found that during the 2008 annual spring bloom dissolved Fe and nutrients are sufficient to support bloom initiation, however its duration and magnitude is primarily set by competition for dissolved Fe between various microbe and phytoplankton groups, which ultimately limits overall production in these waters. In contrast, relatively little is known on the biological fractionation of Si-isotopes by diatoms in New Zealand surface waters. Instead, a majority of the processes relating to variations in $\delta^{30}Si$ in $Si(OH)_4$ and diatom derived BSi in the region are inferred from previous studies in the Southern Ocean and Equatorial Pacific e.g. (Beucher et al., 2008; de Souza et al., 2012a; Fripiat et al., 2012). At present, the only studies investigating Si-isotopes in New Zealand waters are for diatoms and sponges collected in the mesopelagic zone south of New Zealand, an area that is more strongly influenced by SAW (Egan et al., 2012; Rousseau et al., 2016; Wille et al., 2010).

The aims of the voyage were to (1) investigate the physicochemical factors driving the longevity, magnitude and termination of the spring phytoplankton bloom, (2) to investigate

trace metal cycling within the bloom, and (3) to relate this mechanistic understanding of environmental controls on bloom dynamics to remotely sensed-trends in phytoplankton blooms across the mesoscale eddy field east of New Zealand (See Ellwood *et al.* 2015 and references therein). The survey drew on the findings from an earlier voyage in September 2008 (FeCycle II), and utilised a mesocosm experiment to investigate pelagic Fe-cycling within the resident phytoplankton community (Boyd et al., 2012; Ellwood et al., 2015; Ellwood et al., 2014). The work presented here is a supporting study that investigated factors driving BSi formation and Si-isotope fractionation within the spring bloom in the convergence zone east of New Zealand. The aim of this work was to investigate whether the fractionation of Si isotopes in subtropical surface waters east of New Zealand are influence by changes in Fe bioavailability as the annual spring bloom develops. To elucidate whether Fe bioavailability and phytoplankton bloom development influence $\delta^{30}Si$, we complemented water column sampling with a large mesocosm (700 L) experiment and smaller (20 L) incubation experiments. Here, we present comparisons of BSi production and Si-isotope ($\delta^{30}Si_{BSi}$) fractionation in the mesocosm with new $\delta^{30}Si_{BSi}$ data from the subtropical-convergence zone.

2. Methods

2.1 Sampling Site and Experimental Design

The present survey (TAN1212) was part of a GEOTRACES process study and took place in a zone of confluence east of New Zealand (approximately 179ºW, 39ºS). The voyage took place between 15 September 2012 (year day 259) and 7 October 2012 (year day 281). Survey methods were similar to those for a previous voyage in September of 2008 (Boyd et al., 2012); where after an initial survey of the eddy, a drogued drifter was deployed at the centre of the eddy to provide the quasi-Lagrangian sampling platform needed to interpret biogeochemical observations of the feature (for further details on eddy formation, see Boyd et al. (2012) and Ellwood et al. (2014)).

Sea surface (0 – 10m depth) samples for BSi and Si-isotopes were collected between days 263 and 279 using the ships underway seawater supply. Sea surface Chl *a* fluorescence, photosystem II (PSII) photochemical efficiency (F_v/F_m), and the effective absorption cross section of PSII (σ_{PSII}) were monitored in real-time using a Chelsea Instruments Fast Repetition Rate (FRR) fluorometer that was plumbed into the ships underway water supply. Periodically,

size-fractionated Chl *a* samples were collected for analysis. Daily sea-surface samples (10m depth) were collected for dissolved macro-nutrients (NO_3^- + NO_2^-, $Si(OH)_4$ and PO_4^{3-}), particulate nitrogen (PON), particulate carbon (POC), and particulate phosphorus (POP) were collected off pre-dawn sampling casts utilising Niskin bottles deployed on a 24 bottle CTD rosette system (SBE 911plus CTD rosette). Samples for bacteria, *Synechococcus*, *Prochlorococcus*, and pico-eukaryote cell enumeration were collected using the procedures described by Hall et al. (2004)

Daily sea-surface samples (10 m depth) for dissolved Fe (DFe) were obtained using a trace metal clean (TM) rosette. Macro-nutrient concentrations were measured in real-time using a micro-segmented flow analyzer (Astoria Pacific International [API300]) with digital detection (Ellwood et al., 2014). Dissolved Fe (DFe) concentrations were determined onboard by flow-injection analysis with chemiluminescence detection of Fe using luminol after Fe pre-concentration on to Toyopearl AF-Chelate-650 M resin (de Jong et al., 1998) and spiking with hydrogen peroxide (Lohan et al., 2006). Samples for DOC were analysed at the National Institute of Water and Atmospheric Research (NIWA) according to APHA method 5310B using a TOC analyser.

A mesocosm experiment was conducted on day 266 using an acid cleaned 1000 L LDPE bag filled with 350 L of surface seawater that was pre-filtered using an acid cleaned 0.2 µm capsule filter (Supor Acropak 200; Pall). Surface seawater was collected in a trace metal clean manner using a tow fish (Ellwood et al., 2014). The main aim of the mesocosm experiment was to mimic Fe cycling of pelagic Fe in the water column (see Ellwood et al. (2015) for more details). Two bags were used, one spiked with 0.2 nmol L^{-1} of the radionuclide ^{55}Fe and a control, spiked with 0.2 nmol L^{-1} of non-radioactive Fe. Both bags were allowed to equilibrate with natural ligands present in the filtered seawater for 12 hours before being inoculated with another 350 L of unfiltered seawater collected using the TM tow fish containing the natural plankton community (Ellwood et al., 2015). The total volume in each bag was 700 L. The bags were incubated on deck for 168 hours at 50% of the ambient light intensity (attenuated with neutral density screening), and kept at ambient seawater temperature by continual surface seawater circulation around the bags. All analyses and observations for the work presented in this study were made on the bag spiked with non-radioactive Fe. The Fe cycling results for the radioactive Fe experiments are were presented by Ellwood et al. (2015).

To determine the influence the addition of Fe in the mesocosm might have on the resident diatom community, and hence BSi production and the fractionation of $\delta^{30}Si_{BSi}$, a smaller microcosm experiment was run in conjunction on day 272. The experiment was run for 96 hours and acted as an Fe-free control. For this experiment, four 20 L low density polyethene cubic containers were filled using unfiltered seawater from the tow fish, with two of the containers spiked with 0.5 nmol L^{-1} of dissolved Fe, and incubated as described for the mesocosm experiment. For the mesocosm and microcosm experiments pre-incubation samples were collected for macro-nutrient concentrations, BSi and Si-isotopes, photosynthetic parameters (fluorescence, F_v/F_m and σ_{PSII}) and POC, PON and POP. The 700 L mesocosm experiment was sampled every 12-24 hours while the 20 L microcosm experiment was only sampled at the end of the 96-hour incubation in order to avoid possible Fe contamination.

2.2 POC, PON , POP and BSi Analysis

Samples for POC and PON analysis were collected by filtering between 500 and 750 mL of seawater through a pre-combusted 25 mm GFF filter (Merck-Millipore), before rinsing with 50 ml of filtered seawater. Filters were stored at -80^{o}C before analysis. Samples for BSi and silicon isotope analysis were collected onto 25 mm 0.4 µm polycarbonate filters (Pall). Surface seawater samples and samples from the mesocosm experiment were collected by filtering 30 – 60 L (for surface seawater) and 10 – 20 L (for mesocosm and microcosm samples) of sample, respectively, through a 142 mm 0.4 µm polycarbonate filter. The filter was immediately placed in a 50 ml polypropylene tube and capped. All filters were stored at -20 ^{o}C prior to analysis. Hydrolysis of the samples for BSi content was carried out by adding 18 ml of 0.5% (w/w) Na_2CO_3 solution to the tubes and heating them to 85 ^{o}C for 2 hr (Paasche, 1980). When cool, each tube was neutralized with 0.5 M HCl to the turning point of methyl orange (pH 3–4), before being made up to 25 mL with deionised water. Silicate concentrations were determined using the molybdenum blue method (Strickland and Parsons, 1972).

2.3 Preparation of samples for determination of δ^{30}Si of BSi

Samples for $\delta^{30}Si_{BSi}$ determination were rinsed from their filters into 2.5 ml Teflon bombs using deionised water. They were then evaporated to dryness at 50 ^{o}C in a drying oven overnight. To remove any organics that may interfere with the analysis; the samples were treated with 1 mL of 30% (v/v) H_2O_2 solution and refluxed for 24 hours at 70 ^{o}C on a hotplate. Following the

oxidation of organics, the lids of the Teflon bombs were removed, and the samples were left to evaporate to dryness before adding 2 mL of 0.5 M NaOH to dissolve the sample. Samples were then left to reflux for 24 hours at 50 ^{o}C. A portion of the sample was removed, neutralised and the silicate concentration determined using the molybdenum blue method (Strickland and Parsons, 1965). Prior to silicon isotope analysis, sodium was removed from the samples using cation exchange chromatography. Twelve cation exchange columns were prepared using modified polypropylene 2.5 mL Pasteur Pipettes loaded with approximately 1 ml Dowex 50W-X8 cation exchange resin (200-400 mesh). Columns were cleaned by passing 0.5 ml of 8% (v/v) hydrofluoric acid (HF) and 3x 0.75 mL of deionised water over the resin. The resin was then protonated with 3x 0.75 mL 4M HCl followed by 3x 0.75 mL deionised water rinses. Each column was loaded with 0.5 mL of sample and then rinsed with 4x 0.75 mL of deionised water to ensure the entire sample was eluted. To minimize contamination, samples were collected in vials that were cleaned using 8% (v/v) HF, before being rinsed with deionised water.

2.4 Determination of $\delta^{30}Si$ in particulate BSi

The δ^{30}Si of diatom BSi was determined according to methods developed by (Wille et al., 2010) using a multi-collector inductively coupled plasma mass spectrometer (MC-ICP-MS) (Finnigan Neptune, Germany) in medium-resolution mode. An ESI-Apex nebulizer fitted with a Teflon inlet system and a demountable torch fitted with an alumina injector was used for sample introduction. We used a standard-sample-standard bracketing technique for data acquisition and reduction (Wille et al., 2010). The δ^{30}Si signal (based on the relative abundance of ^{30}Si to ^{28}Si (^{30}Si/^{28}Si) was calculated using the following formula:

$$\delta^{30}Si = \left\lfloor \left(\frac{R_{Sample}}{R_{Std}} \right) - 1 \right\rfloor \times 1000 \qquad (1)$$

Where R_{sample} is the ^{30}Si/^{28}Si ratio of the sample and R_{Std} is the ^{30}Si/^{28}Si ratio of the in-house RC11 diatomaceous standard. Measured δ^{30}Si and the δ^{29}Si values were then converted to be relative to the NBS28 reference standard based on the daily offset between the in-house RC11 diatomaceous standard and NBS28. The overall offset between the in-house standard and the NBS28 standard was -2.28 ± 0.14 (n = 11; mean ± 2x standard deviation). Measurements of

sample blanks were made prior to each run to ensure that the combined blank and background was <1% of the total sample signal. NBS28 and the "Diatomite" standard detailed in Reynolds et al. (2007) were also prepared with each daily run, and were measured with every three samples (≤ 8 diatomite/NBS28 standards per daily run). The $\delta^{30}Si$ composition of the "Diatomite" standard (again relative to NBS28) produced average values for $\delta^{29}Si$ of 0.73 ± 0.11 ‰ and $\delta^{30}Si$ of 1.42 ±0.17 ‰ (2 SD, n = 11), and are within the upper 90% confidence range ($\delta^{29}Si$ = 0.79 ‰, $\delta^{30}Si$ = 1.54 ‰) of the modal values ($\delta^{29}Si$ = 0.66 ‰, $\delta^{30}Si$ = 1.27 ‰) from inter-laboratory comparisons performed by Reynolds et al. (2007).

Sample $\delta^{30}Si$ and the $\delta^{29}Si$ values were plotted against each other to ascertain the best-fit mass-dependent fractionation line (MDF, Figure 1). Our calculated slope for the best-fit MDF line was 0.55 with a regression error of 0.13 (2SE, n = 11) and is consistent with the consensus slope of 0.511 obtained from inter-laboratory silicon standard measurements (Figure 1). This value agrees with the slope of the theoretical fractionation line for Si of 0.5092 (Reynolds et al., 2007).

Silicon isotope fractionation in diatoms has been modelled using both closed and open steady-state models (Cardinal et al., 2007; De La Rocha et al., 1997; Varela et al., 2004). The closed system model is employed when there is no net import or export of $Si(OH)_4$ or BSi out of surface waters during the period of biological incorporation of Si (Varela et al., 2004); for example, during periods of intense water column stratification where mixing across the density interface separating the surface mixed layer from deeper waters is minimal (Brzezinski et al., 2001). Because the mesocosm experiment has no inputs or outputs, a closed system model can be used to define the evolution of $\delta^{30}Si$ through the following relationships:

$$\delta^{30}Si(OH)_4 = \delta^{30}Si(OH)_{4\,initial} + \varepsilon \ln f \quad (2)$$

$$\delta^{30}Si_{BSi.inst} = \delta^{30}Si(OH)_4 + \varepsilon \quad (3)$$

$$\delta^{30}Si_{BSi.acc} = \delta^{30}Si(OH)_{4\,initial} - \varepsilon(f \ln f / 1 - f) \quad (4)$$

Where $\delta^{30}Si(OH)_4$ is the isotopic composition of $Si(OH)_4$ in seawater, $\delta^{30}Si(OH)_{4initial}$ is the initial isotopic composition of $Si(OH)_4$ in seawater prior to biological incorporation of $Si(OH)_4$, $\delta^{30}BSi_{inst}$ and $\delta^{30}BSi_{acc}$ are the instantaneous BSi product and accumulated BSi product

(respectively), and f is the fraction of $Si(OH)_4$ remaining in the system after BSi formation ($[Si(OH)_4]/[Si(OH)_{4initial}]$) (Varela et al., 2004). The Rayleigh isotope fractionation model assumes a constant value for α (the fractionation factor), also known as the enrichment factor (ε), where $\varepsilon\ (‰) \approx (1 - \alpha) \times 1000$).

3. Results

3.1 Surface water data

Phytoplankton bloom initiation commenced with a shoaling of the mixed layer on day 272 and continued until the end of the voyage on day 279, with surface fluorescence (Arbitrary units, AU) ranging from < 0.5 prior to bloom formation, to 1.0 after the bloom (Figure 2A). Nitrate and DFe concentrations exhibit 1.5 – 3 fold decreases in surface concentrations during bloom initiation (Figures 2B, 3 and 4A), with NO_3^- concentrations decreasing from >4.8 μmol L^{-1} on day 267 to < 2.3 μmol L^{-1} on day 278, and DFe concentrations decreasing from > 0.3 nmol L^{-1} on day 267 to < 0.2 nmol L^{-1} on days 278 and 279. Silicic acid concentrations were relatively low (< 2 μmol L^{-1}) in comparison to NO_3^- (≤ 5 μmol L^{-1}) during the voyage and exhibited little variation during bloom initiation (Figure 4A).

From the start of the voyage, the phytoplankton community composition in surface waters was dominated by eukaryotic pico-phytoplankton (0.2 – 2 μm in size) and prokaryote pico-phytoplankton (*Synechococcus* and *Prochlorococcus*) (Figure 4B). Pico-eukaryotic plankton cell numbers increased relative to the other plankton groups, exhibiting a 2-fold increase on day 270 and a 3-fold increase by day 279. In comparison, both *Synechococcus* and *Prochlorococcus* populations exhibit little variation between days 263 and 273. *Synechococcus* and *Prochlorococcus* populations change rapidly, however, following day 273, where they exhibit 5-fold and 8-fold increases in their respective populations between days 273 and 279. The pico-phytoplankton also dominated the Chl *a* estimates of phytoplankton biomass (Figure 4D). Night-time measurements of F_v/F_m average around 0.4 between days 263 and 272 before dropping to around 0.3 by day 274 (Figure 4B), following the decline in dissolved Fe concentration (Figure 4A). Between days 274 and 278, F_v/F_m remained around 0.3.

Surface elemental ratios and POC, PON and BSi concentrations are presented in Figure 4, while surface values for $\delta^{30}Si$ from BSi are presented in Table 1. BSi concentrations remained consistent at 0.07 ± 0.02 μmol L^{-1} for the duration of the voyage and displayed little variation despite a relative increase in concentration at the onset of the bloom, from 0.049 μmol L^{-1} on day 273 to 0.103 μmol L^{-1} on day 276 (Table 1, Figure 4C). The lack of variation in surface BSi is reflected in the relatively small change in surface $Si(OH)_4$ concentrations over the duration of the voyage (Figure 4A). Particulate organic nitrogen exhibits a 2-fold increase on day 273 (Figure 4C), which is concomitant with a relative decrease in the surface NO_3^- concentration of ~1.3 μmol L^{-1} (Figure 4A). Samples for $\delta^{30}Si_{BSi}$ from BSi were taken

prior to bloom initiation on days 268 and 270 and exhibited $\delta^{30}Si_{BSi}$ values of 1.61 ± 0.2 ‰ and 1.83 ± 0.2 ‰, respectively (Figure 2B, Table 1), whereas $\delta^{30}Si_{BSi}$ values were relatively lighter with respect to ^{30}Si following bloom initiation, with $\delta^{30}Si_{BSi}$ values of 1.35 ± 0.2 ‰ on day 275, and 1.22 ± 0.2 ‰ on day 279, respectively.

3.2. Mesocosm (700 L bag) experiment

There was a significantly different response in the mesocosm experiment compared to the response in surface waters over the duration of the voyage. Fluorescence and F_v/F_m increased with peak fluorescence at around 160 hr (Table 2 Figure 5A). BSi, NO_3^- and $Si(OH)_4$ concentrations in the bag at the start of the experiment were comparable to sea-surface concentrations of BSi, NO_3^- and $Si(OH)_4$ on day 266, when the experiment was initiated. Both NO_3^- and $Si(OH)_4$ concentrations exhibited an 11-fold and 9-fold decrease (respectively) by the end of the mesocosm experiment, while BSi concentrations increased from 0.1 μmol L^{-1} to 1.3 μmol L^{-1} by the end of the mesocosm experiment (Figure 5B). There was almost complete utilisation of the $Si(OH)_4$ pool in the mesocosm by siliceous organisms, with BSi production reaching 18 ± 1 nmol L^{-1} hr^{-1} during the exponential phase of growth. This value closely resembles the rate of $Si(OH)_4$ depletion in the mesocosm, which reached 20 ± 1 nmol L^{-1} hr^{-1} during the exponential phase of growth.

The starting value $\delta^{30}Si_{BSi}$ for BSi in the mesocosm experiment was 1.49 ± 0.2 ‰ (t = 0 hr) and comparable to the sea-surface $\delta^{30}Si_{BSi}$ value of 1.61 ± 0.2 ‰ collected on day 268 (Figure 5B). Over the course of the mesocosm experiment, $\delta^{30}Si_{BSi}$ values became heavier with respect to ^{30}Si, with $\delta^{30}Si_{BSi}$ values increasing to 2.64 ± 0.2 ‰ by the end of the experiment (Figure 5B). Silicon isotope fractionation within the experiment closely resembled Rayleigh fractionation kinetics, and a fractionation factor (α) of 0.9989, and an initial $\delta^{30}Si_{DSi}$ value of 2.92 ± 0.1 ‰ was calculated by fitting a model to the $\delta^{30}Si_{BSI}$ for BSi (Figure 5C) (De La Rocha et al., 1997). While no phytoplankton community data were available for the mesocosm experiment, examination of late exponential populations confirmed the presence of the diatoms *Asterionelopsis glacilis*, *Mellosira moniliformis* and *Ceratium arcticum* (Figure 6).

3.3.Microcosm (20 L) experiment

Derived photosynthetic parameters from the microcosm experiment are presented in Figure 7. Despite the increase in Chl *a* fluorescence at the end of the experimental period in both control and Fe-addition experiments, both F_v/F_m and Chl *a* concentration decreased in the control experiment, whilst Chl *a* concentration and F_v/F_m increased ($p < 0.05$) in response to Fe-

addition (Figure 7A, Table 3). The PSII effective absorption cross-section (σ_{PSII}) decreased in both treatments by the end of the experimental period, however, this decrease was more pronounced in the Fe-addition experiment. BSi concentration increased from 0.1 μmol L^{-1} at T=0 to 0.9 ±0.2 μmol L^{-1} and 1.1 ±0.1 μmol L^{-1} at T=96 in the control and Fe-addition experiments, respectively. The increase in BSi concentration is consistent with the mesocosm (700 L bag experiment, Figure 7) which exhibited a 12-fold increase in BSi concentration at the end of the experimental period. In addition, both POC and PON concentrations exhibited a 2 – 3 fold increase at the end of the experimental period (Figure 7B), with POC responding more strongly to Fe-addition in comparison to the control experiment. As a result, both treatments exhibited significant increases in elemental ratios at the end of the experimental period (Figure 7C). The increase in the C:N ratio, however, was more pronounced in the Fe-addition treatment, where POC concentration increased 3-fold compared to a 2.4-fold increase in the control. Increases in Si:N and Si:C ratios were due to a more pronounced increase in BSi concentrations compared to increases in PON and POC concentrations. The addition of dissolved Fe appeared had little effect ($p > 0.1$) on the Si:N and Si:C ratios at the end of the experimental period (Figure 7C).

4. Discussion

Here we first discuss the silicic acid, BSi and silicon isotope results from the mesocosm and microcosm experiments. We then place the experiments into context by comparing the findings with water column measurements. We then detail the processes that might regulate silicic acid utilisation in the waters east of New Zealand.

The fractionation of Si isotopes in the mesocosm bag experiment closely resembled Rayleigh fractionation closed-system kinetics as $Si(OH)_4$ was drawdown (Figure 5B). BSi concentration increased 12-fold in the mesocosm over 8 days resultant from increased in diatoms production thus leading to an increase in $\delta^{30}Si_{BSi}$. The value for $\delta^{30}Si_{BSi}$ at the beginning of the mesocosm experiment was 1.49 ± 0.2 ‰, which closely resembled surface values for $\delta^{30}Si_{BSi}$ measured prior to bloom initiation on days 268 and 270 (Figure 5, Table 1). As the experiment progressed $\delta^{30}Si_{BSi}$ increased to 2.64 ± 0.2 ‰ by the end of the experiment. Based on the increase in $\delta^{30}Si_{BSi}$ and the drawdown in silicic acid as the mesocosm bag experiment progressed, we were able to calculate a fractionation factor (α) of 0.9989 (ε = -1.1 ‰) and a starting seawater value for $\delta^{30}Si_{DSi}$ of 2.92 ± 0.1 ‰. The fractionation factor reported from the mesocosm experiment closely resembles fractionation factors previously published for laboratory and field communities. De La Rocha et al. (1997) obtained a value for ε of -1.1 ± 0.4 ‰ for the diatoms *Thalassiosira weisfloggii*, *Thalassiosira sp.* and *Skeletonema costatum* cultured in the laboratory and found that fractionation was independent of species or temperature. More recently Sutton et al. (2013), however, found significant variations in ε between the Southern Ocean species *Chaetoceros brevis* (-2.09 ± 0.09 ‰) and *Fragilariopsis kergulensis* (-0.56 ± 0.07 ‰)., The fractionation factor reported here (-1.13 ± 0.1 ‰) from the mesocosm experiment also closely resembles fractionation factors reported for field communities, e.g. Varela et al. (2004)(-1.2 ±0.2 ‰), Fripiat et al. (2011)(−1.0 ± 0.3‰) suggesting that species composition of the overall diatom community in the open ocean plays an important role in governing the Si isotope composition in surface waters.

The high $\delta^{30}Si_{DSi}$ value calculated from the mesocosm experiment reflects the relatively high $\delta^{30}Si_{BSi}$ values observed at the start of the experiment and also reflects the surface water composition prior to bloom initiation on days 268 and 270 (Figure 5, Table 1). The calculated $\delta^{30}Si_{DSi}$ of 2.92 ± 0.1 ‰ from the experiment is within the range expected for sub-tropical and tropical water (Beucher et al., 2008) and matches those reported from the Polar Frontal Zone of the Pacific Sector of the Southern Ocean (~3.2 ‰) (de Souza et al., 2012b).

In contrast to the mesocosm experiment, changes to $Si(OH)_4$ and BSi concentrations for surface waters within the eddy were relatively subtle (Figure 2B). In contrast to mesocosm experiment, sea-surface values for $\delta^{30}Si_{BSi}$ were relatively constant between days 268 and 270 and then decline by about ~0.5 ‰ though to day 279, following bloom initiation (Table 1). The surface water values presented here on days 275 and 279 for $\delta^{30}Si_{BSi}$ resemble values reported for waters north of the Sub-tropical front in the Atlantic sector of the Southern Ocean (1.30 ± 0.1 ‰)(Fripiat et al., 2012). It is likely that the observed shift in the $\delta^{30}Si_{BSi}$ composition in surface waters towards lighter Si isotopes could be attributable to a change in the supply of $Si(OH)_4$ to surface waters, possibly from SAW (Figure 2B). It also reflects the open system nature of the area.

In contrast to the mesoscom experiment the BSi concentration in surface waters varied little during the ~17 day voyage, only increasing from 0.05 μmol L^{-1} on Day 264 to 0.11 μmol L^{-1} on day 278 (Figure 4C). The relatively rapid uptake of $Si(OH)_4$ in the mesocosm experiment as well as the 12-fold increase in BSi concentrations, in contrast to lack of *in situ* BSi production, suggest that changes in water-column stability may have encouraged more rapid bloom initiation compared to surface waters. It is possible that Fe had a small stimulatory effect within the mesocosm experiment, although it was only increased by 0.2 nmol L^{-1} relative to surface waters, which were 0.3-0.4 nmol L^{-1}. This was tested in smaller microcosm (20 L) experiments, where the rate of BSi production show little variation between control and Fe-addition replicates (p >0.05). In these smaller experiments, Fe addition did seem to affect photosynthetic parameters (F_v/F_m, σ_{PSII} and Chl *a* fluorescence) as well as POC concentration in comparison to the control experiment such that some community dynamics may have differed in the mesocosm experiment compared to the community in surface waters. It is possible that the small addition of Fe may have removed resource competition between diatoms and other phytoplankton in the mesocosm experiment, however, it is more likely that the larger phytoplankton were initially dominating before being run into nitrate and possibly Fe-limitation (Boyd et al., 2012; Ellwood et al., 2015; Ellwood et al., 2014).

The surface water plankton community was dominated by the presence of eukaryotic picoplankton (0.2 – 2 μm), and a background population of photosynthetic prokaryotes (*Synechococcus* and *Prochlorococcus*). Size-fractionated Chl *a* distribution suggests that the picoplankton community dominated photosynthetic biomass. Previous studies in the area also suggest that at its peak, the phytoplankton bloom is dominated by photosynthetic prokaryotes and large diatoms such as *Asterionellopsis glacilalis* (cell volume ~ 60 μm^3) and

Leptocylindrus sp. (~ 600 μm^3) (Boyd et al., 2012). Similarly, we observed an increased abundance of *A. glacialis*, *M. moniliformis* and *C. arcticum* in the exponential stage population in the mesocosm experiment, but not for our water column measurements.

At this stage it is difficult to determine why $Si(OH)_4$ was depleted in the mesocosm, whilst the sea-surface inventory was maintained. The consumption of $Si(OH)_4$ and the formation of BSi in the mesocosm experiment suggests that $Si(OH)_4$ is not the ultimate factor limiting diatom productivity as the water column stratifies and the spring bloom progresses (Boyd et al., 2012). Ultimately the lack of bloom formation in the present study is likely due to water column instability and unfavourable Fe and light supply conditions for bloom initiation (Chiswell et al. submitted), as well as a dominant diatom phytoplankton assemblage compared to picoplankton. Zooplankton grazing may also be suppressed in the mesocosm experiment, which may allow full nutrient and Fe consumption, although during spring bloom development primary producers tend to outcompete grazers (Boyd et al., 2012). For the current study, a fully developed spring bloom did not occur at this site, even after the voyage was competed (Chiswell et al. submitted); there is a hint of a potential iron limitation of the plankton community whereby F_v/F_m declined from 0.4 to 0.3 following a decline in dissolved Fe concentration (Figure 4), so perhaps this was contributing factor to the lack of bloom development.

One of the more important findings of the study was that despite the large species-level variability in Si isotope fractionation factors observed by Sutton et al. (2013), the community level fractionation factor of -1.1 ‰ determined in in this study agrees well with previous estimates of -1.2 ‰ (observed by Fripiat et al. 2012), and -1.1 ‰ (observed by De la Rocha et al. 1997). Furthermore, the fractionation factor that was obtained from the mesocosm experiment appears to exhibit little variation despite the relatively low ambient $Si(OH)_4$ concentrations of 2 $\mu mol\ L^{-1}$ (compared to the Southern Ocean waters, where Si concentrations can be >20 $\mu mol\ L^{-1}$) (de Souza et al., 2012b; Frank et al., 2003). This highlights the utility of the diatom $\delta^{30}Si$ as a proxy for diatom $Si(OH)_4$ utilisation in paleo-reconstructions (e.g. Beucher et al., 2007; De La Rocha et al., 1998) and that species level variation in Si isotope fractionation may not be important when considering past trends in diatom $Si(OH)_4$ utilisation.

4.3. Conclusions

Contrasting results between the mesocosm (700 L) bag experiment and sea-surface measurements suggest that $\delta^{30}Si_{BSi}$ in surface waters rarely exceeds ~ 2 ‰ as a result of Fe-limitation of the diatom population at the end of a phytoplankton bloom (Boyd et al., 2012); and the continuous re-supply of $Si(OH)_4$ to surface waters. Despite this, $\delta^{30}Si_{DSi}$ values in subtropical surface waters east of New Zealand are relatively high, and it is likely that silicic acid resupply by waters enriched in ^{30}Si likely plays a larger role in governing the $\delta^{30}Si$ composition of surface waters, in addition to biological fractionation by diatoms. We also observed that the community level Si isotope fractionation factor is independent of species composition and $Si(OH)_4$ concentration. Our observed value of -1.1 ‰ is also consistent with previous field studies (Fripiat et al. 2012 and Varela et al. 1997) and similar to mono-specific lab culture studies (De la Rocha et al. 1997 and Milligan et al. 2004).

5. Acknowledgements

This work was funded by the New Zealand Government through a grant to NIWA. We acknowledge the Australian Research Council for financial support (DP110100108, DP0770820, and DP130100679) and the Natural Environmental Research Council (NERC NE/H004475/1 awarded to Maeve Lohan to support AM). Thank Gregory de Souza and an anonymous reviewer for helpful comments that helped to improve the manuscript.

Table 1. Surface BSi concentrations and δ^{30}BSi values over the duration of the voyage. Duplicate samples for BSi were taken on days 266, 268 and 270 (mean ± 1 SD). $\delta^{29}Si_{BSi}$ and $\delta^{30}Si_{BSi}$ values are per mil (‰) with errors based on 2 standard deviation calculated from multiple measurements.

Longitude/Latitude	Day	Date	$\delta^{29}Si_{BSi}$	$\delta^{30}Si_{BSi}$	Surface BSi concentration (μmol L^{-1})
179.14 W 39.09 S	263	19/09/2012			0.092
179.15 W 39.07 S	264	20/09/2012			0.084
179.15 W 39.07 S	265	21/09/2012			0.074
179.17 W 39.02 S	266	22/09/2012			0.091 ± 0.050
179.24 W 38.58 S	267	23/09/2012			0.055
179.29 W 38.58 S	268	24/09/2012	0.82 ± 017	1.61 ± 0.25	0.073 ± 0.010
179.30 W 38.58 S	269	25/09/2012			0.040
179.27 W 39.10 S	270	26/09/2012	0.96 ± 0.17	1.83 ± 0.25	0.071 ± 0.010
179.34 W 38.50 S	271	27/09/2012			0.056
179.40 W 38.52 S	272	28/09/2012			0.049
179.40 W 39.04 S	273	29/09/2012			0.049
179.38 W 38.52 S	274	30/09/2012			0.046
179.56 W 38.28 S	275	01/10/2012	0.66 ± 0.17	1.35 ± 0.25	0.045
179.53 W 38.28 S	276	02/10/2012			0.102
179.58 W 38.59 S	277	03/10/2012			0.088
179.45 W 39.04 S	278	04/10/2012			0.110
179.49 W 38.60 S	279	05/10/2012	0.60 ± 0.17	1.22 ± 0.25	0.092

Table 2. Results from the mesocosm (700 L bag) experiment for BSi, NO_3^- and $Si(OH)_4$, the isotope composition ($\delta^{30}Si_{BSi}$) of BSi, fluorescence, and F_v/F_m.

Time (hr)	BSi (µmol L^{-1})	$\delta^{30}Si_{BSi}$ (‰)	$Si(OH)_4$ (µmol L^{-1})	NO_3 (µmol L^{-1})	F_o	F_v/F_m
0	0.091	1.49			2.40	0.06
22					1.90	0.19
24	0.042	1.62	1.88	4.78		
36	0.049	1.94				
38			1.94	4.77		
46					1.80	0.23
48	0.087					
51			1.95	4.70		
58					2.00	0.23
61			1.87	4.58		
72	0.157				2.30	0.23
75			1.81	4.44		
94					3.20	0.35
96	0.332	2.04				
98			1.74	3.53		
118					7.10	0.36
120	0.542	2.19				
122			1.16	2.50		
144	0.750	2.54			12.8	0.26
146			0.82	1.55		
166					13.2	0.27
168	1.29	2.64				
170			0.47	0.42		
190					12.8	0.24
194			0.28			

Table 3. Values from microcosm (20 L) experiment at T = 0 hours and at T = 96 hours (n ≥ 3, 1 S.D). BSi, Si:N and Si:C values with no error (*) reflect the single BSi measurement taken at T= 0 hours prior to the start of the experiment.

Parameter	T = 0 hr	Control (T = 96 hr)	Fe-addition (T = 96 hr)
Chl *a* fluorescence	3.95 ±0.1	9.12 ±0.4	8.62 ±0.5
F_v/F_m	0.38 ±0.02	0.35 ±0.01	0.41 ±0.01*
σPSII	762 ±61	717 ±35	595 ±41*
Chl a (mg L^{-1})	1.34 ±0.1	1.26 ±0.1	1.75 ±0.1†
POC (µmol L^{-1})	10.2 ±0.5	24.7 ±1.1	31.6 ±2.5†
PON (µmol L^{-1})	1.6 ±0.01	3.24 ±0.2	3.22 ±0.2
BSi (µmol L^{-1})	0.1*	0.92 ±0.2	1.09 ±0.1
Si:N (mol/mol)	0.06*	0.28 ±0.05	0.34 ±0.03
Si:C (mol/mol)	0.01*	0.04 ±0.001	0.03 ±0.004
C:N (mol/mol)	6.38 ±0.23	7.64 ±0.09	9.8 ±0.18‡

*Variation from control at the 90-95 % confidence interval

†Variation from control at the 95-99% confidence interval

‡Variation from control at >99% confidence interval

References

Baines, S.B., Pace, M.L., 1991. The production of dissolved organic matter by phytoplankton and its importance to bacteria: Patterns across marine and freshwater systems. Limnology and Oceanography 36, 1078-1090.

Beucher, C.P., Brzezinski, M.A., Jones, J.L., 2008. Sources and biological fractionation of Silicon isotopes in the Eastern Equatorial Pacific. Geochim. Cosmochim. Acta 72, 3063-3073.

Bostock, H.C., Sutton, P.J., Williams, M.J.M., Opdyke, B.N., 2013. Reviewing the circulation and mixing of Antarctic Intermediate Water in the South Pacific using evidence from geochemical tracers and Argo float trajectories. Deep-Sea Research Part I: Oceanographic Research Papers 73, 84-98.

Boyd, P., LaRoche, J., Gall, M., Frew, R., McKay, R.M.L., 1999. Role of iron, light, and silicate in controlling algal biomass in subantarctic waters SE of New Zealand. Journal of Geophysical Research-Oceans 104, 13395-13408.

Boyd, P.W., Strzepek, R., Chiswell, S., Chang, H., DeBruyn, J.M., Ellwood, M., Keenan, S., King, A.L., Maas, E.W., Nodder, S., Sander, S.G., Sutton, P., Twining, B.S., Wilhelm, S.W., Hutchins, D.A., 2012. Microbial control of diatom bloom dynamics in the open ocean. Geophys. Res. Lett. 39, L18601.

Boyd, P.W., Strzepek, R.F., Ellwood, M.J., Hutchins, D.A., Nodder, S.D., Twining, B.S., Wilhelm, S.W., 2015. Why are biotic iron pools uniform across high- and low-iron pelagic ecosystems? Global Biogeochemical Cycles 29, 1028–1043.

Brzezinski, M.A., Dumousseaud, C., Krause, J.W., Measures, C.I., Nelson, D.M., 2008. Iron and silicic acid concentrations together regulate Si uptake in the equatorial Pacific Ocean. Limnology and Oceanography 53, 875-889.

Brzezinski, M.A., Nelson, D.M., Franck, V.M., Sigmon, D.E., 2001. Silicon dynamics within an intense open-ocean diatom bloom in the Pacific sector of the Southern Ocean. Deep Sea Res. Pt II 48, 3997-4018.

Brzezinski, M.A., Pride, C.J., Franck, V.M., Sigman, D.M., Sarmiento, J.L., Matsumoto, K., Gruber, N., Rau, G.H., Coale, K.H., 2002. A switch from $Si(OH)_4$ to NO_3^- depletion in the glacial Southern Ocean. Geophys. Res. Lett. 29, doi:10.1029/2001GL014349.

Butler, E.C.V., Butt, J.A., Lindstrom, E.J., Tildesley, P.C., Pickmere, S., Vincent, W.F., 1992. Oceanography of the subtropical convergence zone around Southern New Zealand. New Zealand Journal of Marine and Freshwater Research 26, 131-154.

Cardinal, D., Savoye, N., Trull, T.W., Dehairs, F., Kopczynska, E.E., Fripiat, F., Tison, J.-L., Andre, L., 2007. Silicon isotopes in spring Southern Ocean diatoms: Large zonal changes despite homogeneity among size fractions. Marine Chemistry 106, 46-62.

Chiswell, S.M., Bostock, H.C., Sutton, P.J.H., Williams, M.J.M., 2015. Physical oceanography of the deep seas around New Zealand: a review. New Zealand Journal of Marine and Freshwater Research, 1-32.

de Jong, J.T.M., den Das, J., Bathmann, U., Stoll, M.H.C., Kattner, G., Nolting, R.F., de Baar, H.J.W., 1998. Dissolved iron at subnanomolar levels in the Southern Ocean as determined by ship-board analysis. Analytica Chimica Acta 377, 113-124.

De La Rocha, C.L., Brzezinski, M.A., DeNiro, M.J., 1997. Fractionation of silicon isotopes by marine diatoms during biogenic silica formation. Geochim. Cosmochim. Acta 61, 5051-5056.

de Souza, G.F., Reynolds, B.C., Johnson, G.C., Bullister, J.L., Bourdon, B., 2012a. Silicon stable isotope distribution traces Southern Ocean export of Si to the eastern South Pacific thermocline. Biogeosciences 9, 4199–4213.

de Souza, G.F., Reynolds, B.C., Rickli, J., Frank, M., Saito, M.A., Gerringa, L.J.A., Bourdon, B., 2012b. Southern Ocean control of silicon stable isotope distribution in the deep Atlantic Ocean. Global Biogeochem. Cycles 26, GB2035.
Egan, K.E., Rickaby, R.E.M., Leng, M.J., Hendry, K.R., Hermoso, M., Sloane, H.J., Bostock, H., Halliday, A.N., 2012. Diatom silicon isotopes as a proxy for silicic acid utilisation: A Southern Ocean core top calibration. Geochim. Cosmochim. Acta 96, 174-192.
Ellwood, M.J., Hutchins, D.A., Lohan, M.C., Milne, A., Nasemann, P., Nodder, S.D., Sander, S.G., Strzepek, R., Wilhelm, S.W., Boyd, P.W., 2015. Iron stable isotopes track pelagic iron cycling during a subtropical phytoplankton bloom. Proceedings of the National Academy of Sciences 112, E15-E20.
Ellwood, M.J., Nodder, S.D., King, A., Hutchins, D.A., Wilhelm, S.W., Boyd, P.W., 2014. Pelagic iron cycling during the subtropical spring bloom, east of New Zealand. Marine Chemistry 160, 18-33.
Fernandez, D., Bowen, M., Carter, L., 2014. Intensification and variability of the confluence of subtropical and subantarctic boundary currents east of New Zealand. Journal of Geophysical Research: Oceans 119, 1146-1160.
Franck, V.M., Bruland, K.W., Hutchins, D.A., Brzezinski, M.A., 2003. Iron and zinc effects on silicic acid and nitrate uptake kinetics in three high-nutrient, low-chlorophyll (HNLC) regions. Marine Ecology Progress Series 252, 15-33.
Fripiat, F., Cavagna, A.-J., Savoye, N., Dehairs, F., André, L., Cardinal, D., 2011. Isotopic constraints on the Si-biogeochemical cycle of the Antarctic Zone in the Kerguelen area (KEOPS). Marine Chemistry 123, 11-22.
Fripiat, F., Cavagna, A.J., Dehairs, F., de Brauwere, A., André, L., Cardinal, D., 2012. Processes controlling the Si-isotopic composition in the Southern Ocean and application for paleoceanography. Biogeosciences 9, 2443-2457.
Hall, J.A., Safi, K., Cumming, A., 2004. Role of microzooplankton grazers in the subtropical and subantarctic waters east of New Zealand. New Zealand Journal of Marine and Freshwater Research 38, 91-101.
Lohan, M.C., Aguilar-Islas, A.M., Bruland, K.W., 2006. Direct determination of iron in acidified (pH 1.7) seawater samples by flow injection analysis with catalytic spectrophotometric detection: Application and intercomparison. Limnology and Oceanography: Methods 4, 164-171.
Marchetti, A., Varela, D.E., Lance, V.P., Johnson, Z., Palmucci, M., Giordano, M., Armbrust, E.V., 2010. Iron and silicic acid effects on phytoplankton productivity, diversity, and chemical composition in the central equatorial Pacific Ocean. Limnology and Oceanography 55, 11.
Meyerink, S., Ellwood, M.J., Maher, W.A., Strzepek, R., 2017. Iron Availability Influences Silicon Isotope Fractionation in Two Southern Ocean Diatoms (Proboscia inermis and Eucampia antarctica) and a Coastal Diatom (Thalassiosira pseudonana). Frontiers in Marine Science 4.
Milligan, A.J., Varela, D.E., Brzezinski, M.A., Morel, F.M.M., 2004. Dynamics of silicon metabolism and silicon isotopic discrimination in a marine diatom as a function of pCO_2. Limnology and Oceanography 49, 322-329.
Murphy, R.J., Pinkerton, M.H., Richardson, K.M., Bradford-Grieve, J.M., Boyd, P.W., 2001. Phytoplankton distributions around New Zealand derived from SeaWiFS remotely-sensed ocean colour data. New Zealand Journal of Marine and Freshwater Research 35, 343-362.
Nodder, S.D., Boyd, P.W., Chiswell, S.M., Pinkerton, M.H., Bradford-Grieve, J.M., Greig, M.J.N., 2005. Temporal coupling between surface and deep ocean biogeochemical processes in contrasting subtropical and subantarctic water masses, southwest Pacific Ocean. Journal of Geophysical Research-Oceans 110.

Nodder, S.D., Northcote, L.C., 2001. Episodic particulate fluxes at southern temperate mid-latitudes (42-45 degrees S) in the Subtropical Front region, east of New Zealand. Deep-Sea Research Part I-Oceanographic Research Papers 48, 833-864.
Paasche, E., 1980. Silicon content of five marine plankton diatom species measured with a rapid filter method. Limnol. Oceanogr 25, 474-480.
Pichevin, L.E., Ganeshram, R.S., Geibert, W., Thunell, R., Hinton, R., 2014. Silica burial enhanced by iron limitation in oceanic upwelling margins. Nature Geosci 7, 541-546.
Reynolds, B.C., Aggarwal, J., André, L., Baxter, D., Beucher, C., Brzezinski, M.A., Engström, E., Georg, R.B., Land, M., Leng, M.J., Opfergelt, S., Rodushkin, I., Sloane, H.J., van den Boorn, S.H.J.M., Vroon, P.Z., Cardinal, D., 2007. An inter-laboratory comparison of Si isotope reference materials. Journal of Analytical Atomic Spectrometry 22, 561-568.
Rousseau, J., Ellwood, M.J., Bostock, H., Neil, H., 2016. Estimates of late Quaternary mode and intermediate water silicic acid concentration in the Pacific Southern Ocean. Earth and Planetary Science Letters 439, 101-108.
Sarmiento, J.L., Gruber, N., Brzezinski, M.A., Dunne, J.P., 2004. High-latitude controls of thermocline nutrients and low latitude biological productivity. Nature 427, 56-60.
Sarmiento, J.L., Simeon, J., Gnanadesikan, A., Gruber, N., Key, R.M., Schlitzer, R., 2007. Deep ocean biogeochemistry of silicic acid and nitrate. Global Biogeochemical Cycles 21, doi:10.1029/2006GB002720.
Smetacek, V., Assmy, P., Henjes, J., 2004. The role of grazing in structuring Southern Ocean pelagic ecosystems and biogeochemical cycles. Antarctic Science 16, 541-558.
Strickland, J.D., Parsons, T.R., 1972. A practical handbook of seawater analysis.
Strickland, J.D.H., Parsons, T.R., 1965. A manual of sea water analysis.
Sutton, J.N., André, L., Cardinal, D., Conley, D.J., de Souza, G.F., Dean, J., Dodd, J., Ehlert, C., Ellwood, M.J., Frings, P.J., Grasse, P., Hendry, K., Leng, M.J., Michalopoulos, P., Panizzo, V.N., Swann, G.E.A., 2018. A Review of the Stable Isotope Bio-geochemistry of the Global Silicon Cycle and Its Associated Trace Elements. Frontiers in Earth Science 5.
Sutton, J.N., Varela, D.E., Brzezinski, M.A., Beucher, C.P., 2013. Species-dependent silicon isotope fractionation by marine diatoms. Geochim. Cosmochim. Acta 104, 300-309.
Varela, D.E., Pride, C.J., Brzezinski, M.A., 2004. Biological fractionation of silicon isotopes in Southern Ocean surface waters. Global Biogeochemical Cycles 18, doi:10.1029/2003GB002140.
Wille, M., Sutton, J., Ellwood, M.J., Sambridge, M., Maher, W., Eggins, S., Kelly, M., 2010. Silicon isotopic fractionation in marine sponges: A new model for understanding silicon isotopic variations in sponges. Earth and Planetary Science Letters 292, 281-289.

Figures

Figure 1. Mass dependent fractionation (MDF) of $\delta^{29}Si$ vs $\delta^{30}Si$ line for all diatom samples relative to NBS28. MDF line represented by $\delta^{29}Si = 0.55 \pm 0.02[\delta^{30}Si] - 0.08 \pm 0.04$, $r^2 = 0$.

Figure 2. A. Underway surface Chlorophyll fluorescence data, measured in arbitrary units (AU) obtained from the FRR (Fast Repetition Rate) Fluorometer for year days 268, 270, 275 and 279 of the voyage. Black dots represent drogue drifter tracks. **B**. Surface (0 - 10m) values for BSi, $Si(OH)_4$, $\delta^{30}Si$ and DFe for year days 268, 270, 275 and 279.

Figure 3. Profiles of DFe, $Si(OH)_4$, NO_3^-, and PO_4^{3-} concentration versus depth for year days 267, 270, 275 and 278.

Figure 4. A Mean surface (0 – 10 m) nutrients ($Si(OH)_4$, NO_3^-, PO_4^{3-} and DFe) over the duration survey. B. cell counts for cyanobacteria and size fractionated eukaryotic phytoplankton along with night-time F_v/F_m measurements. C. Concentrations of POC, PON and BSi. D. Size fractionated Chlorophyll *a* concentrations and the Chl:C ratio. For surface macro-nutrients ($Si(OH)_4$, NO_3^- and PO_4^{3-}), values are in µmol L^{-1} ±1SD (n = 2). For mean DFe concentrations, values are in nmol L^{-1}, ±1SD ($n \geq 4$).

Figure 5. Results from the mesocosm (700 L bag) experiment; **A.** Photosynthetic parameters **B** Concentrations of BSi, NO_3^- and $Si(OH)_4$ and the isotope composition ($\delta^{30}Si_{BSi}$) of BSi over the experimental period; **C**. Variation in $\delta^{30}Si_{BSi}$ during the experimental period, where f is the fraction of dissolved silicon remaining (Si/Si_0, where Si_0 is the starting concentration of $Si(OH)_4$ in the bag). Instrumental errors for $\delta^{30}Si$ values are 0.2 ‰ (2SE). A fractionation factor (α) of 0.9989 was calculated using a SOLVER based algorithms to fit a model (equation 4) to the data and closely resembles the reported fractionation factor (ε) of -1.2 ± 0.02 ‰ for diatoms in the field (Fripiat et al., 2011). Also present is the model (equation 2) for evolution of $\delta^{30}Si(OH)_4$ during the experiment.

Figure 6. Microscope images of *Asterionelopsis glacilis* and *Mellosira moniliformis*. *A. glacilis* is a pennate diatom (general length, 30 – 150 µm), while *M. moniliformis* is a centric diatom (Length, 11-30 µm, diameter, 17 – 70 µm).

Figure 7. Change in **A.** photosynthetic parameters B. POC, PON and BSi concentration C. and elemental ratios for microcosm (20 L) experiment harvested after 96 hours incubation time. Experiments represents T0, control and Fe-addition experiments.

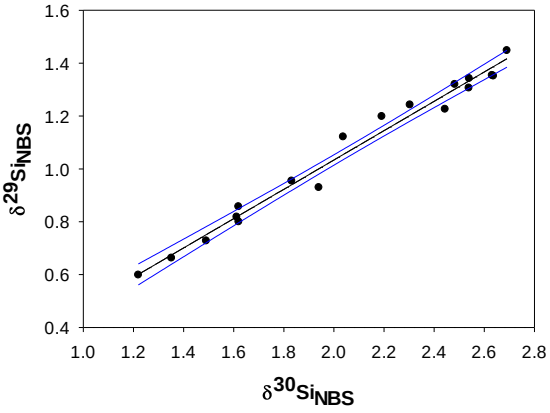

652

653

654

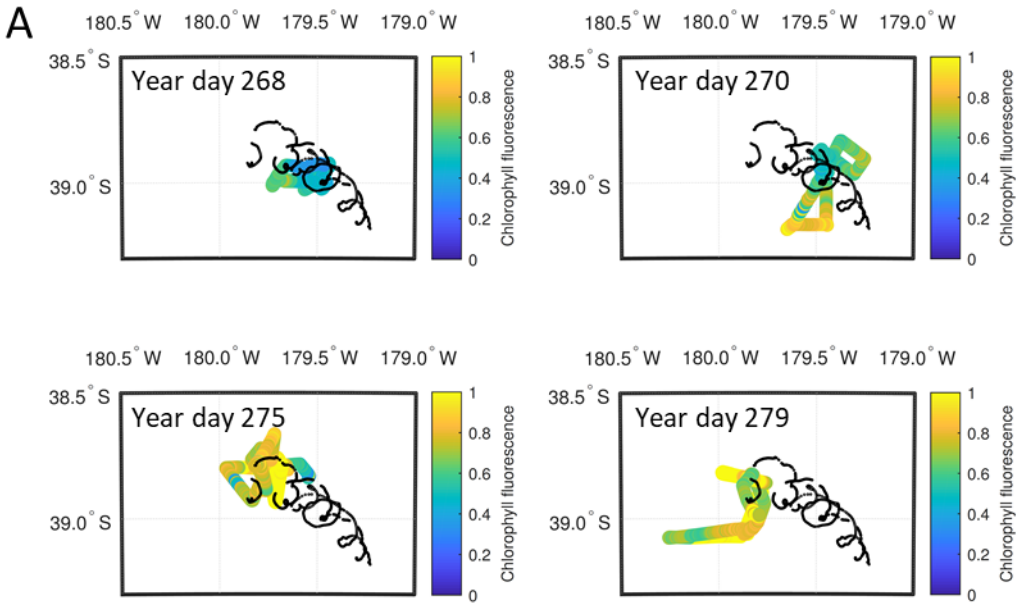

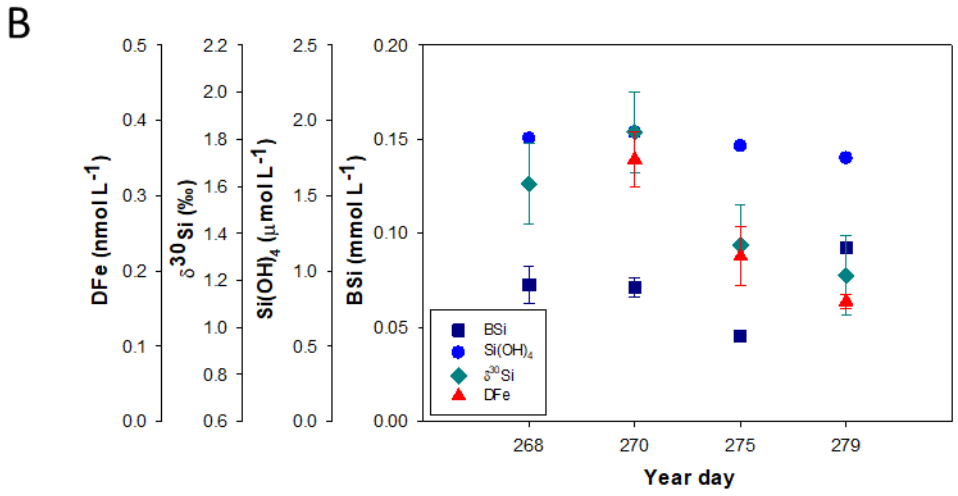

655

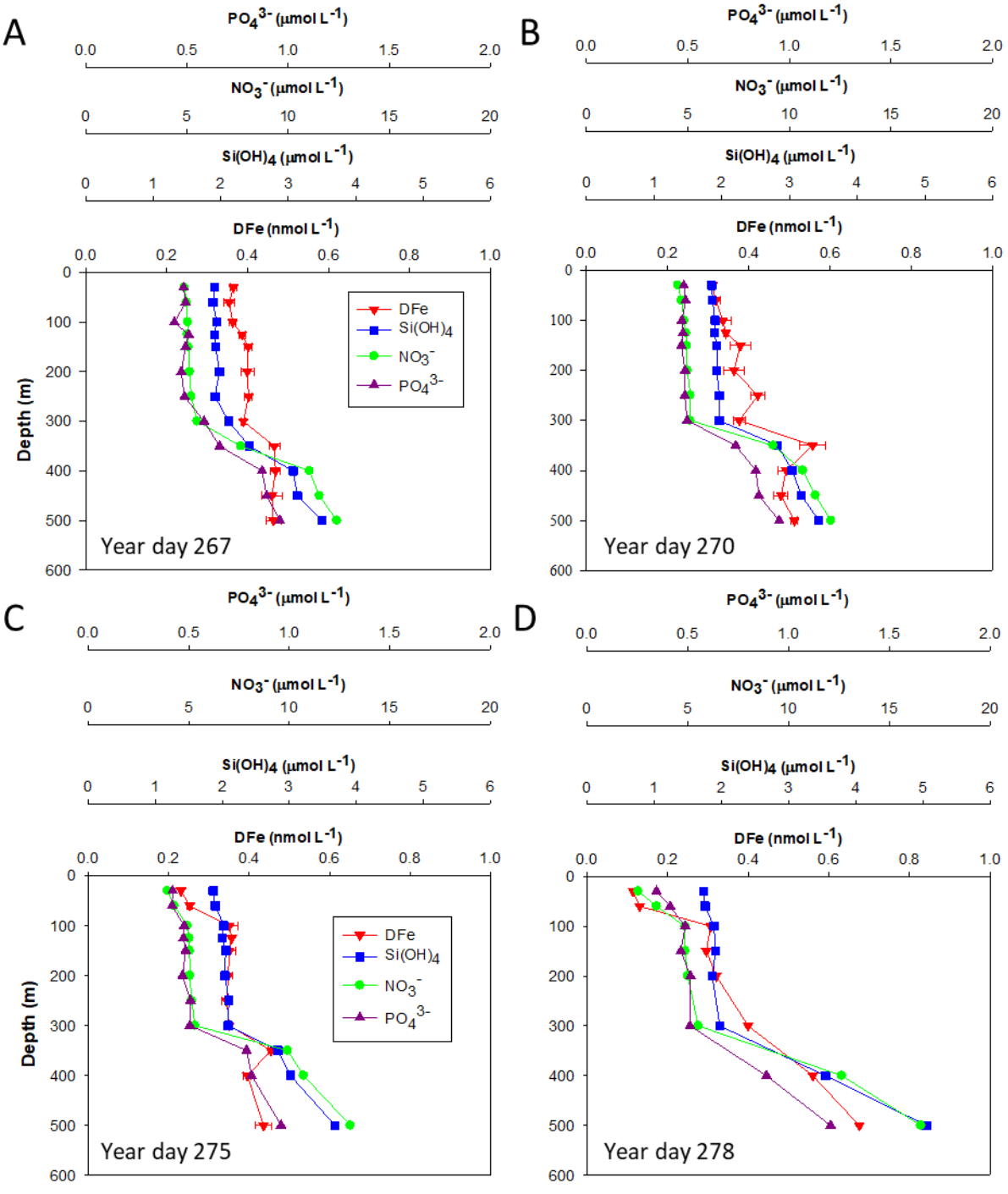
A
B
C
D
PO_4^{3-} (µmol L^{-1})
NO_3^- (µmol L^{-1})
$Si(OH)_4$ (µmol L^{-1})
DFe (nmol L^{-1})
Depth (m)
DFe
$Si(OH)_4$
NO_3^-
PO_4^{3-}
Year day 267
Year day 270
Year day 275
Year day 278

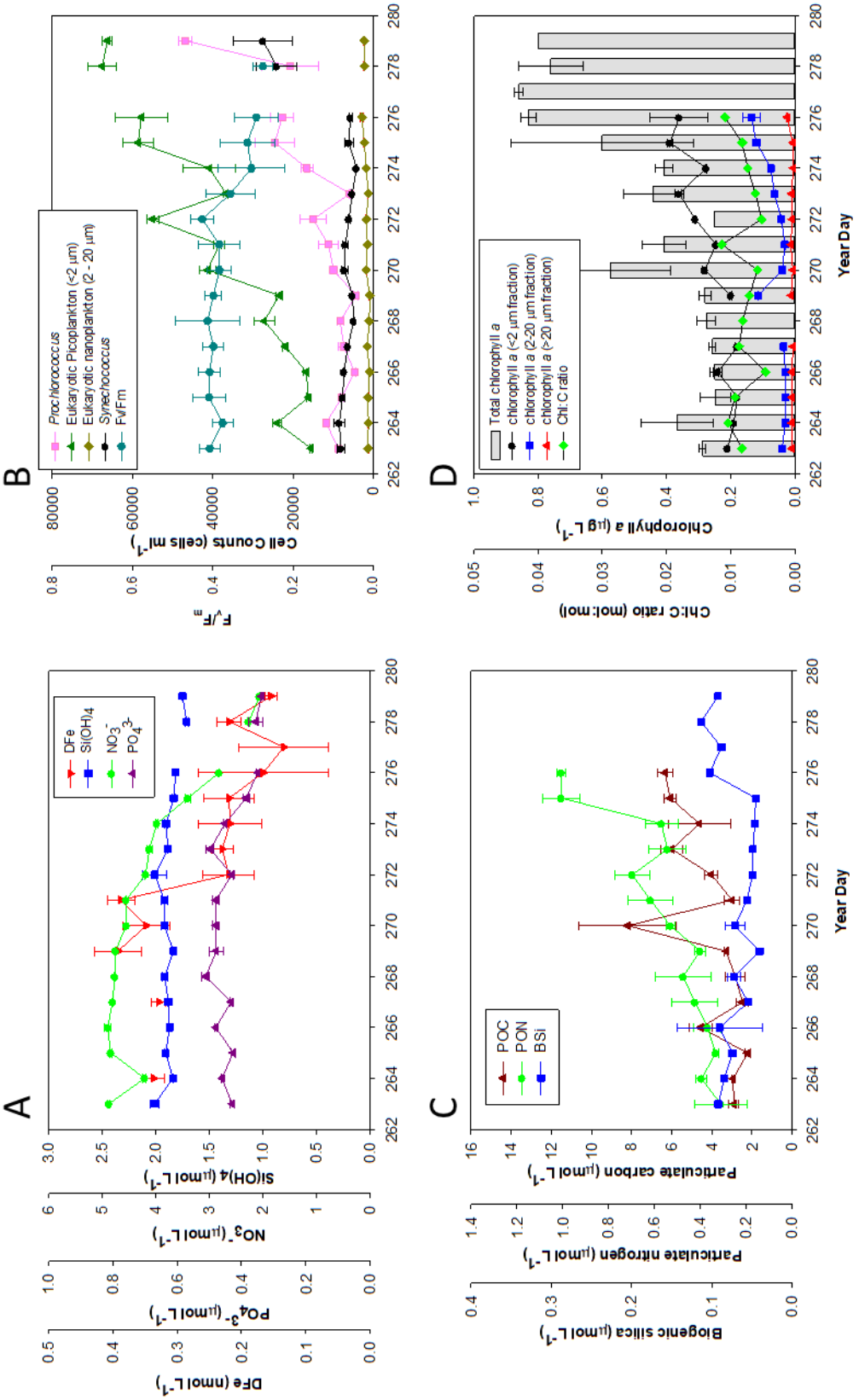
A
B
C
D
DFe
Si(OH)4
NO3-
PO43-
Prochlorococcus
Eukaryotic Picoplankton (<2 µm)
Eukaryotic nanoplankton (2 - 20 µm)
Synechococcus
FvFm
Total chlorophyll a
chlorophyll a (<2 µm fraction)
chlorophyll a (2-20 µm fraction)
chlorophyll a (>20 µm fraction)
Chl:C ratio
POC
PON
BSi
Year Day

662

663

664

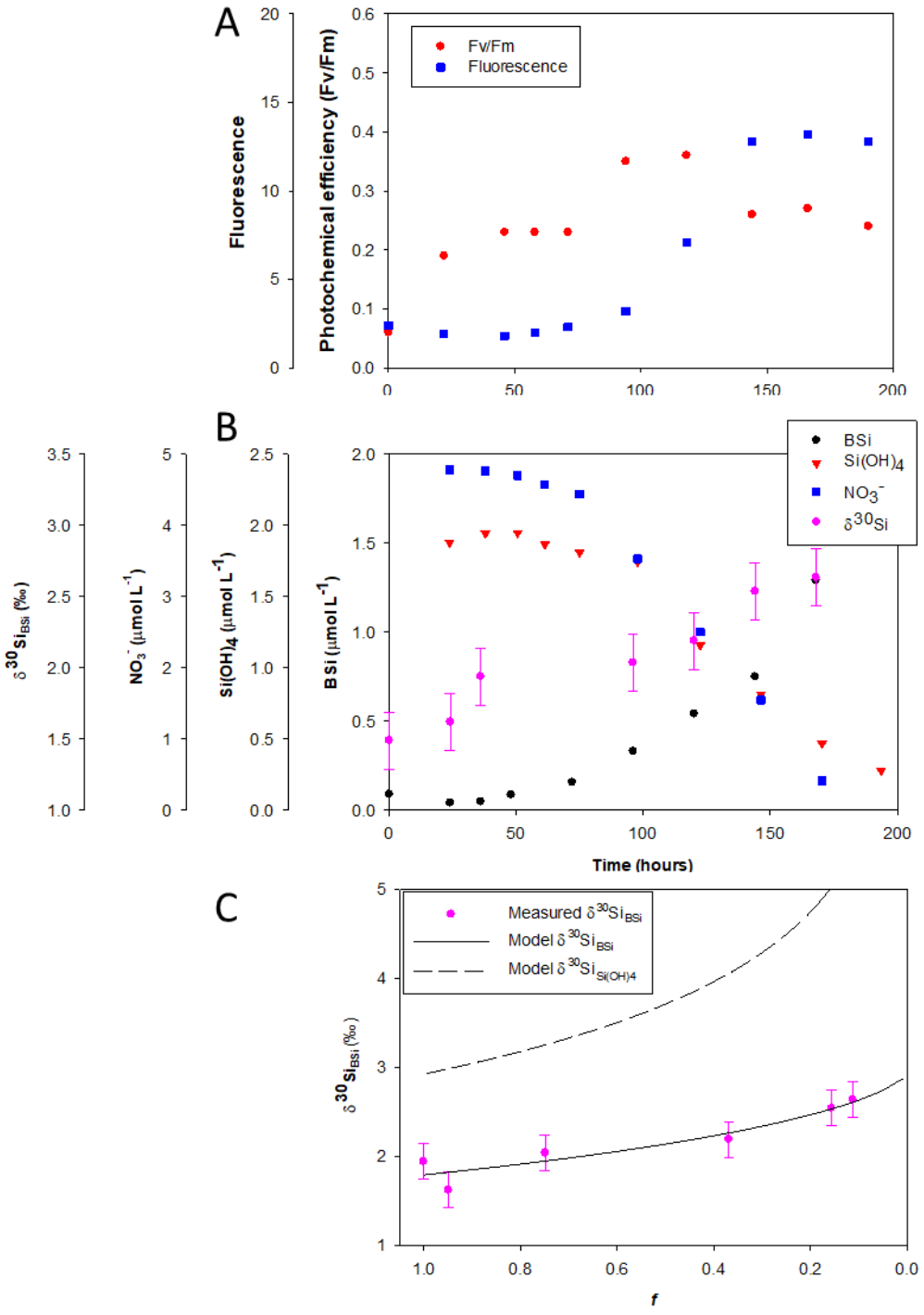

665

666

667

668

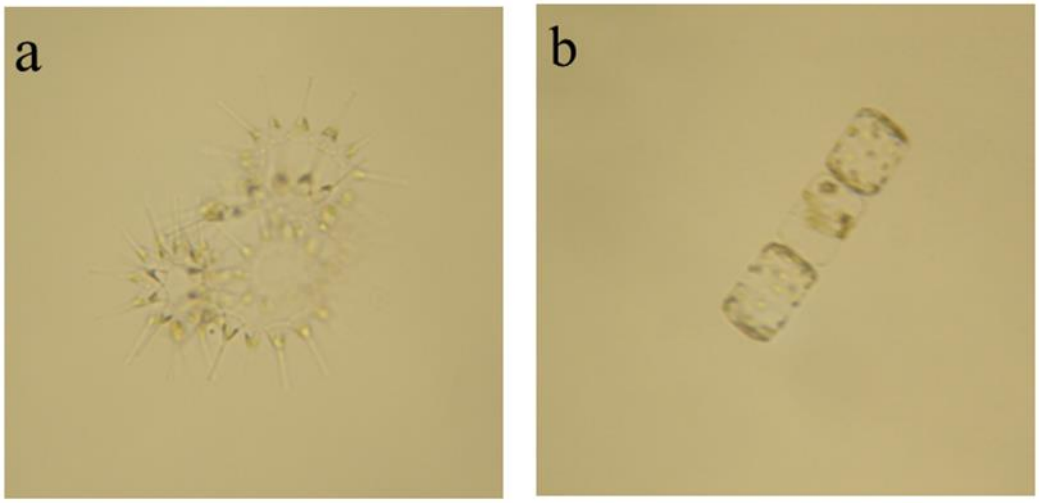

669

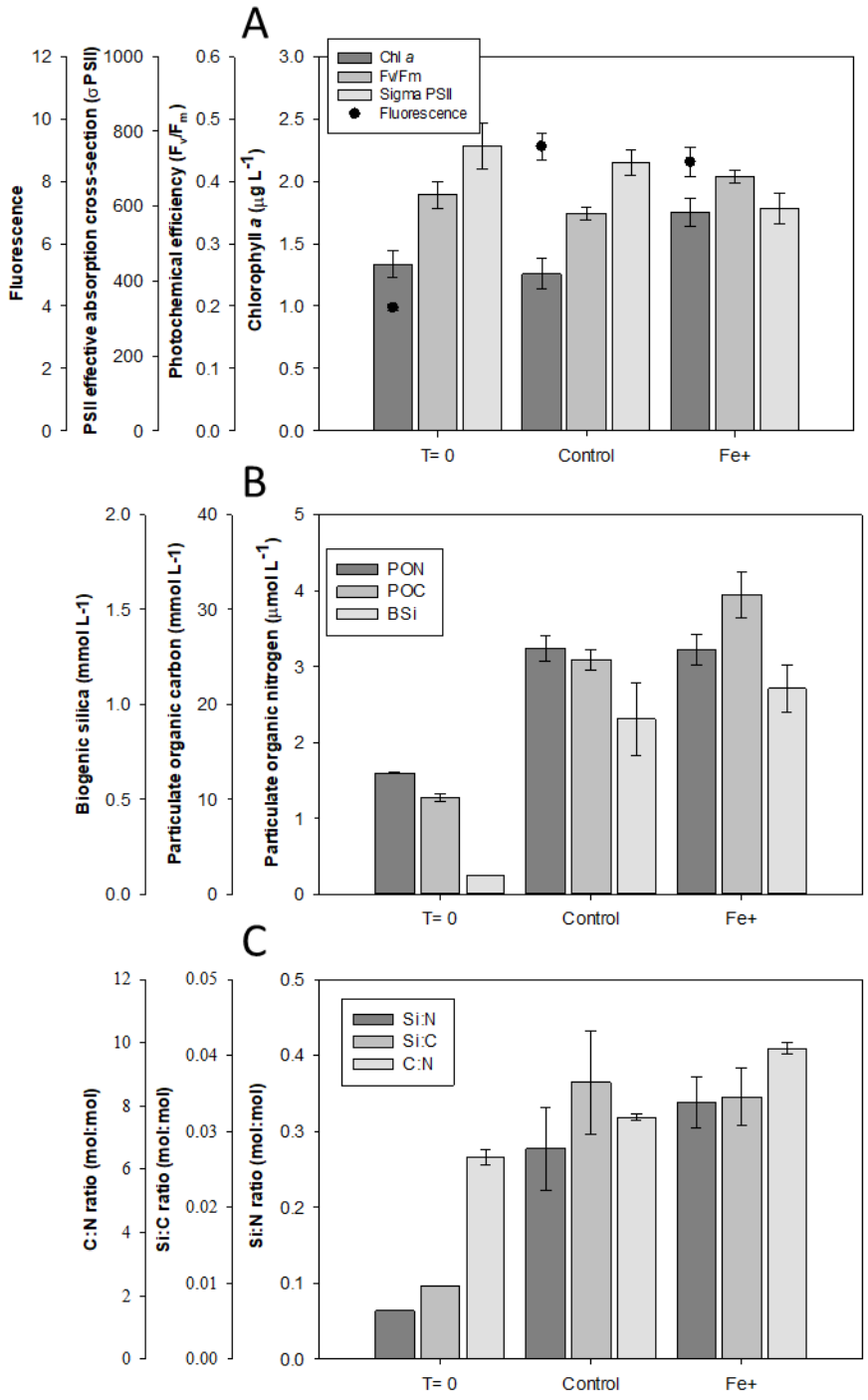
A
Fluorescence
PSII effective absorption cross-section (σPSII)
Photochemical efficiency (Fv/Fm)
Chlorophyll a (µg L-1)
Chl a
Fv/Fm
Sigma PSII
Fluorescence
T= 0
Control
Fe+
B
Biogenic silica (mmol L-1)
Particulate organic carbon (mmol L-1)
Particulate organic nitrogen (µmol L-1)
PON
POC
BSi
T= 0
Control
Fe+
C
C:N ratio (mol:mol)
Si:C ratio (mol:mol)
Si:N ratio (mol:mol)
Si:N
Si:C
C:N
T= 0
Control
Fe+

670